




Narrow Bandgap Photocatalysts for High-Efficiency Renewable Hydrogen Production

Prof. Gregory F. Metha	Prof. Paul A. Maggard	Prof. Vladimir B. Golovko
 THE UNIVERSITY <i>of</i> ADELAIDE		 UC UNIVERSITY OF CANTERBURY <i>Te Whare Wānanga o Waitaha</i> CHRISTCHURCH NEW ZEALAND

Introduction

Decarbonising the world's energy sector is the most significant way to curb CO₂ emissions. Photocatalysis is an emerging technology for producing a green fuel, hydrogen, from water and sunlight. An efficient visible light photocatalyst contains three key components.

1. A narrow bandgap
2. Cocatalyst decorations
3. Efficient electronic structure

The perovskite photocatalyst Ba_{0.6}Sn_{0.4}Zr_{0.5}Ti_{0.5}O₃ (BSZT) with a bandgap of 2.34 eV (in the visible light region) satisfies component 1. Consequently, this project has been focused on components 2 and 3.

Previous Results (from Progress Report)

Previously, Au₉ clusters were loaded onto BSZT to act as co-catalysts for hydrogen production. High resolution TEM images of Au₉/BSZT and other size-specific gold clusters were obtained. The former proved Au₉ clusters surface decorated BSZT. However, despite a modified synthesis, the formation of a Sn (tin) outer domain was observed. This domain could impede charge migration to the cocatalyst if not carefully controlled. To address this concern the Sn shell has now been studied in detail and additional co-catalysts investigated.

Investigating the Sn Shell in Ba_{0.6}Sn_{0.4}Zr_{0.5}Ti_{0.5}O₃

The tin layer in BSZT was comprehensively characterized by combining *in situ* powder X-ray diffraction, TEM of FIB-sliced images, computational modelling and Mössbauer spectroscopy.

The molecular structure of the Sn layer is integral to the charge separation efficiency of the BSZT particle. By combining Mössbauer spectroscopy (which probes the Sn oxidation state) with TEM, it was found that Sn is primarily incorporated into BSZT as size-tuneable SZT nanoshells. These shells are surrounded by a small layer of tin oxide (Figure 1). This means that the previously observed Sn outer domain actually comprises two different structures. Overall, BSZT particles comprise three domains: BZT (core), SZT (shell) and SnO₂ (outer layer) (Figure 1).

The perovskite lattice, confirmed for both BZT and SZT, is demonstrably efficient for charge transfer. Consequently, the formation of SZT nanoshells may facilitate photocatalysis. Computational modelling suggests a mechanism in which photogenerated holes in the BZT core

are preferentially driven to the more energetic valence band of the SZT shell, enhancing charge separation (**Figure 1**).

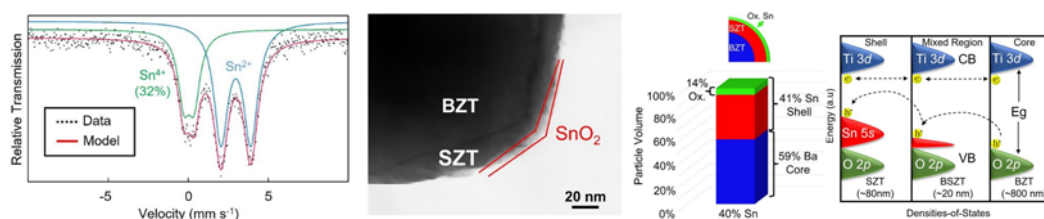


Figure 1: Characterisation techniques identifying the formation of SZT nanoshells. (left) BSZT ^{119}Sn Mössbauer spectra. (middle left) BSZT TEM image identifying three domains. (middle right) calculated molar fractions of the three domains. (right) densities-of-states diagrams of the BSZT valence band and conduction band.

BSZT can be further optimised by determining ideal formation properties of the SZT shell, e.g. shell thickness. Suppressing formation of the SnO_2 layer is also beneficial. More broadly, improvements to charge separation, identified in core-shell BZT-SZT, may be advantageous to other perovskite photocatalysts.

Study of Additional Co-catalysts

Concurrent to the investigation into BSZT, other methods of optimising Au clusters were studied. Photocatalytic activity for Au_9/BSZT was not observed, indicating Au_9 may not be suitable for hydrogen production. Further, clusters can agglomerate during photocatalysis, limiting activity. In light of these factors, reduced graphene oxide (rGO) was coupled with Au_{101} clusters on the photocatalyst, $\text{Al}:\text{SrTiO}_3$.

$\text{Au}_{101}/\text{rGO}/\text{Al}:\text{SrTiO}_3$, along with various control samples was fabricated, characterised and tested for photocatalytic H_2 production. The two samples which had both rGO and Au_{101} (red and orange data points) dramatically outperformed all the control samples (purple to yellow data points) (**Figure 2**). The improved activity was only evident when both components, i.e. Au_{101} and rGO, were present. This stems from two properties.

1. Improved migration of the photogenerated electrons from the photocatalyst to the cocatalyst
2. Reduced agglomeration of the clusters during photocatalysis

Regarding the first point, rGO is a demonstrated conductive mediator. Evidence for the latter point was provided by TEM. A comparison of Au_{101} cluster size before and after photocatalysis, indicates that minimal agglomeration was induced during photocatalysis (**Figure 2**).

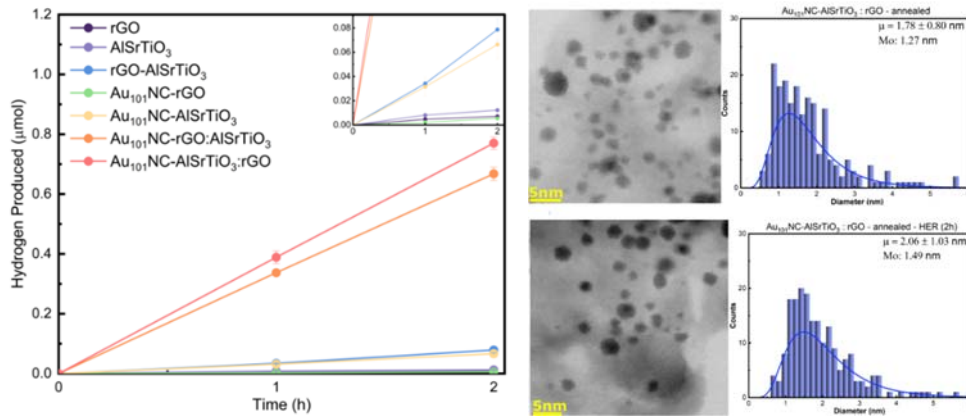


Figure 2: (left) Photocatalytic H_2 production of various samples TEM of Au_{101} clusters on rGO wrapped Al:SrTiO₃ with a size distribution histogram. (top right) before photocatalysis. (bottom right) after photocatalysis.

Conclusion

Comprehensive characterisation of BSZT identified a core-shell BZT-SZT structure which could improve hole separation to redox active sites and improve electronic structure efficiency. Meanwhile, cocatalyst studies on another perovskite, Al:SrTiO₃, identified electronic coupling of the Au_{101} cluster via rGO. This method reduces photocatalytic agglomeration and improves electron separation. Consequently, the two pathways facilitating hole and electron separation respectively could show improved H_2 production from sunlight when combined. The three lead investigators have agreed to pursue this research direction and will be seeking additional funds to undertake this new work.